

Effects of Camera Alignment Errors on Stereoscopic Depth Estimates

Wenyi Zhao¹ and N. Nandhakumar²

Machine Vision Laboratory, Dept of Electrical Engineering
University of Virginia, Charlottesville VA 22903

¹Email: wz4a@virginia.edu ²Email: nn7e@virginia.edu

Summary

We present in this paper a new analysis of relative sensitivity/importance of camera calibration/alignment parameters on the performance of stereoscopic depth reconstruction. For a given stereoscopic vision system, once stereo correspondence is successfully established, the accuracy of 3D measurements depends on the overall geometric structure of the model in relation to object distances. The geometric structure (and hence the error) depends on (1) fixed design parameters such as interpixel distance, focal length and baseline; and (2) the accuracy with which these parameters are known, i.e., camera calibration and alignment. The errors due to the fixed design parameters of the geometric structure have been investigated intensively by others. However, the role of calibration error and misalignment on the accuracy of the stereoscopically computed 3D information has not been studied. The alignment accuracy is perhaps more important than individual camera calibration since it is the relative alignment that affects the epipolar constraints used during the correspondence process. Also, poor camera calibration/alignment may affect the establishment of feature/region correspondence at the outset. Most research done in camera calibration has dealt with the question of how to calibrate a single camera or multiple cameras, and also on the derivation of error bounds of different calibration parameters. But in many situations, it may be very difficult to get perfect calibration. Further, even if the calibration is excellent, the camera setting may change during the use of the system. This raises two important questions: How do these calibration/alignment errors affect 3D estimates? Given the accuracy requirements that a practical, application-specific stereoscopic vision system must satisfy, how much error can we endure for each parameter we calibrate?

The quantitative analysis presented here provides formulae which relate different calibration or alignment parameter errors to the 3D reconstruction measurements. The results of this analysis provide specifications of acceptable tolerances in individual calibration parameters for given 3D measurement error tolerances. This information is useful in designing practical stereoscopic vision systems.

Effects of Camera Alignment Errors on Stereoscopic Depth Estimates *

Wenyi Zhao and N. Nandhakumar

Machine Vision Lab, Dept of Electrical Engineering, Univ. of Virginia
Charlottesville VA 22903

Abstract: We present in this paper a new analysis of relative sensitivity/importance of camera calibration/alignment parameters on the performance of stereoscopic depth reconstruction. This quantitative analysis provides formulae which relate different parameter errors to the 3D reconstruction measurements. The results of this analysis provide specifications of acceptable tolerances in individual calibration parameters for given 3D measurement error tolerances. This information is useful in designing practical stereoscopic vision systems.

KEYWORDS Stereoscopic Vision Camera Calibration/Alignment

1 Introduction

Camera calibration is a very important issue that must be addressed when developing a practical stereoscopic vision system. For a given stereoscopic vision system, once stereo correspondence is successfully established, the accuracy of 3D measurements depends on the overall geometric structure of the model in relation to object distances. The geometric structure (and hence the error) depends on (1) fixed design parameters such as interpixel distance, focal length and baseline; and (2) the accuracy with which these parameters are known, i.e., camera calibration and alignment. The errors due to the fixed design parameters of the geometric structure have been investigated intensively by others. However, the role of calibration error and misalignment on the accuracy

*Supported by a research contract from Simpson Weather Associates, Inc., and by the NSF under grant IRI-91109584.

of the stereoscopically computed 3D information has not been studied. The alignment accuracy is perhaps more important than individual camera calibration since it is the relative alignment that affects the epipolar constraints used during the correspondence process. Also, poor camera calibration/alignment may affect the establishment of feature/region correspondence at the outset.

Most research done in camera calibration has dealt with the question of how to calibrate a single camera or multiple cameras, and also on the derivation of error bounds of different calibration parameters. This has prompted a great deal of research in developing methods for camera calibration^[1-7]. But in many situations, it may be very difficult to get perfect calibration. From a practical point of view, camera alignment is critical to stereo-based 3D measurements. Further, even if the calibration is excellent, the camera setting may change during the use of the system. This raises two important questions: How do these calibration/alignment errors affect 3D estimates? Given the accuracy requirements that a practical, application-specific stereoscopic vision system must satisfy, how much error can we endure for each parameter we calibrate?

In this paper we do *not* present a new method of camera calibration. Instead, we analyze the effect of various calibration errors on the performance of a stereoscopic vision system. The analysis provides insight on the relative importance of various calibration/alignment parameters, and quantifies these relationships. Past analysis of calibration has followed one of the following approaches: (1) analysis of 3D measurement errors due to image plane quantization^[8-10], (2) analysis of 3D measurement error due to false correspondences^[11], and (3) analysis of single camera movement errors^[12]. However, such past work lacks detailed analysis of how the individual calibration/alignment parameter error influences the accuracy of the 3D stereoscopic measurements.

The analysis we will present is important because even with the most exacting camera calibration and/or alignment techniques, there will always exist some errors, either large or tiny. It

is important to understand which individual errors have the greatest impact on the accuracy of the stereoscopically computed 3D information. This will assist system designers in placing closer calibration tolerances on the more significant sources of error.

2 Effects of Calibration Errors

Let us consider a binocular vision system with two cameras mounted on some rigid support (figure 1). Ideally, we would like the two cameras to have the same orientation, their optical axes being perpendicular to the long axis of the bar and each individual camera being calibrated perfectly.

In the following discussion, we first consider each source of error separately, *i.e.*, when we discuss one source of error, all other factors are assumed *perfect*. Then we consider the composite effects of several error sources. We assume that we always find the *correct* match between the corresponding image primitives in the stereo image pair. The sources of error we consider may be grouped into the following five categories. The first three of these are phenomena associated with a two-camera system, while the last two are phenomena associated with a single-camera system:

Binocular Error Effects:

1. Depth error due to rotation/roll between two cameras.
2. Depth error due to pitch between two cameras.
3. Depth error due to yaw between two cameras.

Monocular Error Effects:

4. Depth error due to nonparallel CCD array and lens.
5. Depth error due to lens distortion.

Figure 1: Binocular vision system with two cameras

2.1 Depth error due to rotation/roll between two cameras

Consider the case where camera 1 is perfectly calibrated and its optical axis is perpendicular to the bar supporting the two cameras (figure 1). Camera 2's optical axis is parallel to that of camera 1. Camera 2 is also perfectly calibrated except for an unknown rotation angle about the optical axis. With simple trigonometry (figure 2), we have the following fundamental equations.

$$D_{\text{tru}} = f\left(\frac{B}{y_2 - y_1} - 1\right) \simeq f\left(\frac{B}{y_2 - y_1}\right) \quad (1)$$

$$D_{\text{obs}} = f\left(\frac{B}{y'_2 - y_1} - 1\right) \simeq f\left(\frac{B}{y'_2 - y_1}\right) \quad (2)$$

where D_{obs} is the *observed* absolute depth from the image plane to the object, D_{tru} is the *true* absolute depth, f is the effective focal length of both cameras (assuming they are the same), B is the baseline, y_i is the true i^{th} camera's image plane coordinate measured from the *piercing point of perfect camera i* along the epipolar line, and y'_i is the corresponding observed value. All measurements are assumed to be in the same units, say *mm*. The approximations indicated above are based on the assumption that $D_{\text{tru}} \gg f$, which is commonly met in practice.

Based on the assumption that camera 1 is perfect, the error in depth is

$$D_{\text{err}} = D_{\text{tru}} - D_{\text{obs}} \quad (3)$$

$$= f\left(\frac{B}{y_2 - y_1} - 1\right) - f\left(\frac{B}{y'_2 - y_1} - 1\right) \quad (4)$$

$$= fB \frac{y_2 - y_2'}{(y'_2 - y_1)(y_2 - y_1)} \quad (5)$$

$$\simeq D_{\text{tru}} \left(\frac{y'_2 - y_2}{y_2 - y_1}\right) \quad (6)$$

Setting $y'_2 = y_2 \cos \theta$, where θ is the rotation/roll angle between the two cameras, and using $y_i = f \frac{Y_i}{D_{\text{tru}} + f}$, where Y_i is the *true* 3D coordinate of the object satisfying $y_i = f \frac{Y_i}{D_{\text{tru}} + f}$ and $Y_2 - Y_1 = B$, we have

$$D_{\text{err}} \simeq D_{\text{tru}} \left(\frac{y'_2 - y_2}{y_2 - y_1}\right) \quad (7)$$

$$\simeq D_{\text{tru}} \frac{Y_2(\cos \theta - 1)}{B} \quad (8)$$

Figure 3 illustrates the behavior of this error term for different values of relative roll and different values of the 3D coordinate, Y_2 , of the object.

2.2 Depth error due to pitch between cameras

Assume that Camera 1 is perfectly aligned with respect to the bar, and the other camera is also perfectly calibrated except that it is not on the same level as camera 1 with respect to the bar and rotates about a line which is parallel to the bar (figure 4(a)). Hence, the epipolar line is no longer parallel to bar. From figure 4(b), we can see the observed image coordinate y'_2 is the length of the line segment (bold) formed by the intersection between the triangular patch $P_i P_0 O'_2$ and the plane

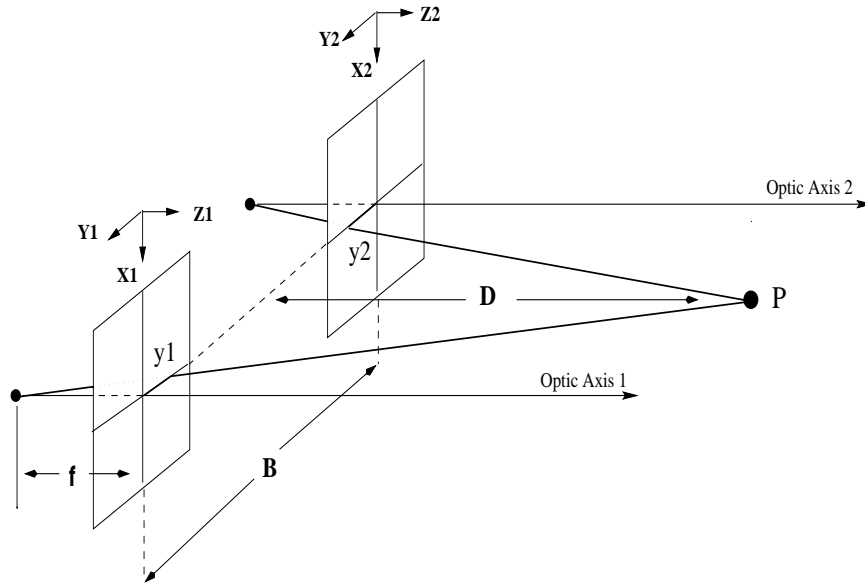


Figure 2: Stereo Fundamentals. Each camera defines its own 3D coordinate frame (X_i, Y_i, Z_i) . The origin of each 3D coordinate frame is located at the intersection of the optic axis and image plane of the corresponding camera. Note that a left handed coordinate frame is used. The 2D image plane coordinates of the point are denoted by (x_i, y_i) .

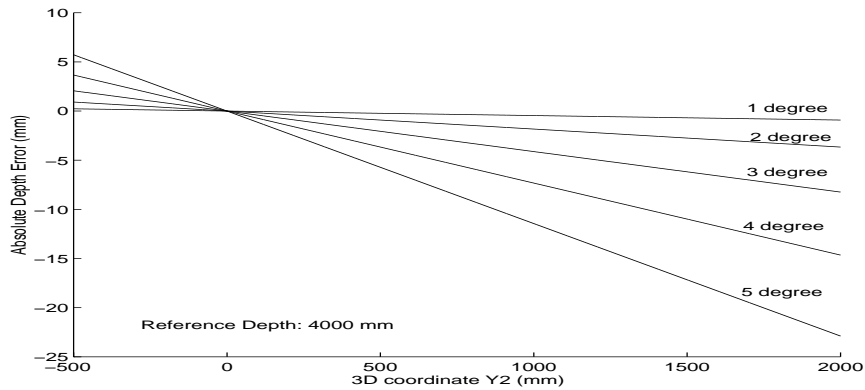


Figure 3: 3D error due to relative roll. Parameters used here: $B = 1330mm, f = 8.5mm$

(a)

(b)

Figure 4: Error due to pitch between cameras. (a) illustrates the relative camera positions (b) shows the stereoscopic geometry.

def , where plane def is perpendicular to the optic axis O'_2P_0 . Using simple trigonometry, we have $y'_2 = y_2 \cos \alpha$, where α is the pitch angle between the two cameras. After this, we could follow the same procedure as we did in case 2.1. Instead, let us use a slightly different procedure here. We know that $\sec \alpha$ is equal to $\sqrt{1 + (\tan \alpha)^2}$, so y'_2 can be obtained from y_2 and α :

$$y'_2 = \frac{y_2}{\sqrt{1 + (\tan \alpha)^2}} \simeq y_2 \left[1 - \frac{1}{2} (\tan \alpha)^2 \right] \quad (9)$$

Noticing that α is usually small, as is $\tan \alpha$, we use Taylor's series to derive the right hand side of the above equation.

Then by using the general equation 6, we have

$$D_{\text{err}} \simeq D_{\text{tru}} \frac{(y_2 [1 - \frac{1}{2} (\tan \alpha)^2] - y_1)}{(y_2 - y_1)} \quad (10)$$

$$\simeq -\frac{1}{2} \frac{y_2 (D_{\text{tru}} \tan \alpha)^2}{fB} \quad (11)$$

$$\simeq -\frac{1}{2} \frac{Y_2 D_{\text{tru}} \tan \alpha^2}{B} \quad (12)$$

(a) (b)

Figure 5: Two special cases: (a) Type I (b) Type II

Now, let us consider two special conditions of this case (Figure 5):

- Type I (Figure 5(a))

- In this condition, $y_2' = \frac{y_2}{\cos \alpha}$. And the final approximation is:

$$D_{\text{err}} \simeq D_{\text{tru}}^2 \frac{y_2 \left(\frac{1}{\cos \alpha} - 1 \right)}{fB} \simeq D_{\text{tru}} \frac{Y_2 \left(\frac{1}{\cos \alpha} - 1 \right)}{B} \quad (13)$$

- Type II (Figure 5(b)):

- The 3D measurement error is 0, provided the assumption of correct correspondence is satisfied.

Figure 6 illustrates the behavior of this error term for different values of relative pitch and different values of the 3D coordinate, Y_2 , of the object.

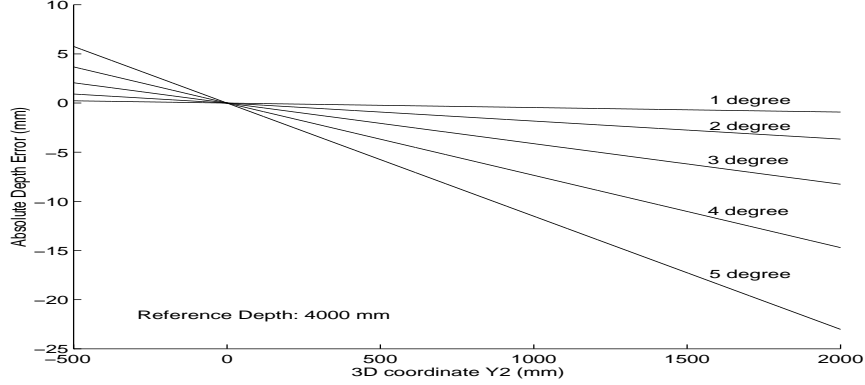


Figure 6: 3D error due to relative pitch. Parameters used here: $B = 1330\text{mm}$, $f = 8.5\text{mm}$

2.3 Depth error due to yaw between cameras

Camera 1 is perfectly aligned with respect to the bar, and the other camera is perfectly calibrated except for an unknown rotation about an axis perpendicular to the epipolar plane and through the center of projection (figure 7). Similar to the above cases, we only need to calculate y'_2 .

From figure 7, we know $v = \beta + \tau$, $\tan v = \frac{y_2}{f}$, and $\tan \tau = \frac{y'_2}{f}$. Employing the trigonometric property: $\tan v = \frac{\tan \beta + \tan \tau}{1 - \tan \beta \tan \tau}$, we have:

$$\frac{y_2}{f} = \frac{\tan \beta + \frac{y'_2}{f}}{1 - \tan \beta \frac{y'_2}{f}} \quad (14)$$

So y'_2 can be expressed as:

$$y'_2 = f \frac{y_2 - f \tan \beta}{y_2 \tan \beta + f} \quad (15)$$

where β is the yaw angle between the two cameras. The approximation equation for D_{err} is:

$$D_{\text{err}} \simeq -\frac{\tan \beta D_{\text{tru}}^2 [1 + (\frac{y_2}{f})^2]}{B} \quad (16)$$

$$\simeq -\frac{\tan \beta (D_{\text{tru}}^2 + Y_2^2)}{B} \quad (17)$$

Figure 7: Error due to yaw between Cameras

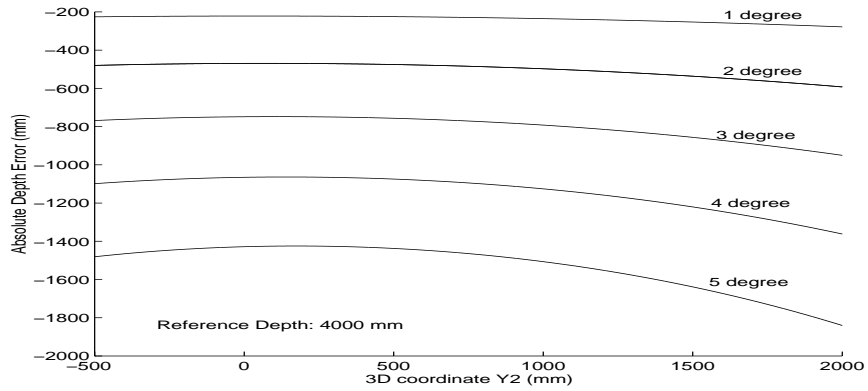


Figure 8: 3D error due to relative yaw. Parameters used here: $B = 1330mm$, $f = 8.5mm$

Although we have used an approximation to derive a simple expression for D_{ERR} , we have found that such an approximation is not as valid as in previous cases. Also since the error in yaw (misalignment) usually contributes most to the error in measured depth, we prefer to use the accurate equation (5) to estimate depth error. The behavior of this error term for different values of relative yaw and different values of the 3D coordinate, Y_2 , of the object is illustrated in figure 8.

2.4 Depth error due to nonparallel CCD array and lens

We assume that both cameras are aligned perfectly with respect to the rigid support. While camera 1 is perfect, the CCD array of camera 2 is not parallel to its lens (figure 9). This is different from section 2.3, where the lens and CCD of each camera were parallel to each other but the optic axes of the two cameras were not parallel.

From figure 9, we have:

$$y_2 = f \tan \psi, \quad \chi = 90^\circ + \phi - \psi \quad (18)$$

where the angle between tilted CCD array and lens is denoted as ϕ , ψ is just the angle between the optic axis and projection ray connecting the object and the lens center, and χ is the angle between this projection ray and tilted CCD array. The latter angles change with the object position.

Using the trigonometric property

$$\frac{\sin \chi}{f} = \frac{\sin \psi}{y_2'} \quad (19)$$

we have the following equation:

$$y_2' = \frac{f \sin \psi}{\cos(\psi - \phi)} \quad (20)$$

For this case, we get depth error D_{err} :

$$D_{\text{err}} \simeq -\frac{D_{\text{tru}}^2}{B} \tan \psi \left[\frac{1}{\cos \phi (1 + \tan \psi \tan \phi)} - 1 \right] \quad (21)$$

$$\simeq -\frac{Y_2^2 \sin \phi}{B} \quad (22)$$

The behavior of this error term for different values of relative tilted angle and different values of the 3D coordinate, Y_2 , of the object is illustrated in figure 10.

Figure 9: Error due to nonparallelism between Lens and CCD Array

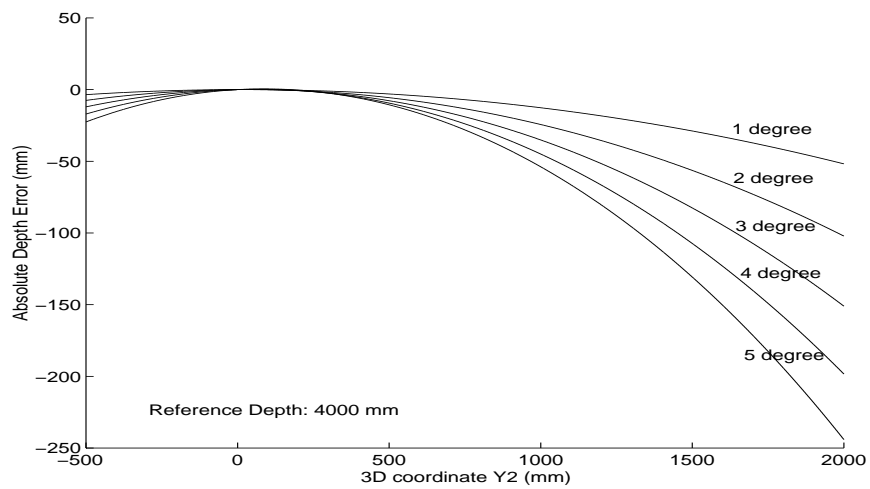


Figure 10: 3D error due to nonparallel CCD and lens. Parameters used here: $B = 1330mm$, $f = 8.5mm$

2.5 Depth error due to lens distortion

We assume that the alignment of both cameras is perfect, and the only error source is due to lens distortion. Adopting the second order radial lens distortion model here^[13], we express y'_1 and y'_2 in terms of y_1, y_2 , and *distortion coefficients* κ_1, κ_2 , as

$$y'_2 - y'_1 = (y_2 - y_1) - (\kappa_2 y_2^3 - \kappa_1 y_1^3) \quad (23)$$

Again in order to maintain accuracy, we will eschew approximations to get depth error from:

$$D_{\text{err}} = fB \left[\frac{1}{y_2 - y_1} - \frac{1}{y'_2 - y'_1} \right] \quad (24)$$

In terms of Y_2 , we have the following equation:

$$D_{\text{err}} = D_{\text{tru}} - \frac{1}{\frac{1}{D_{\text{tru}}} - \frac{f^2}{D^3 B} [\kappa_2 Y_2^3 - \kappa_1 (Y_2 - B)^3]} \quad (25)$$

In figure 11, we plot the depth error introduced by the lens distortion for different values of the 3D coordinate Y_2 , of the object at different depths.

2.6 Relative Importance of Calibration Parameters

Based on the above results, it is easy to tell which parameter needs more attention in calibration/alignment. The most critical parameter is the relative yaw between cameras, followed by the tilt of the CCD array, and then pitch and roll. Also, it is easy to compute the individual calibration/alignment tolerances given some desired system performance. For example, for a given vision

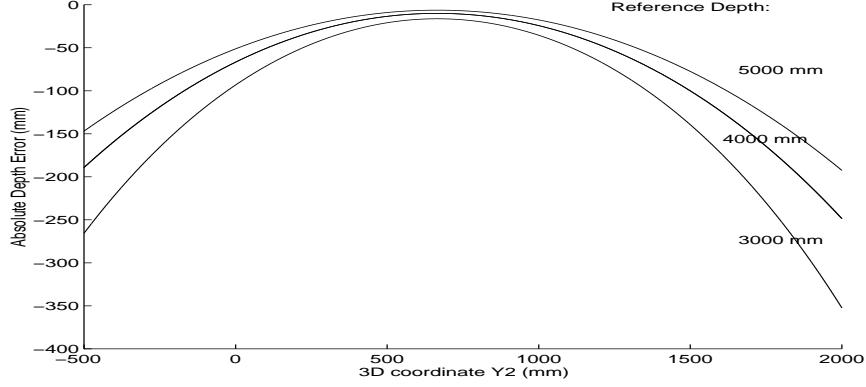


Figure 11: 3D error due to lens distortion. Parameters used here: $B = 1330mm$, $f = 8.5mm$, and $\kappa_i = 0.00231mm^{-2}$ which is obtained experimentally using Tsai's algorithm

system with $B = 1330mm$, $f = 8.5mm$, if we want the depth error to be less than $30mm$ for a point with depth $D_{tru} = 4000mm$ and $Y_2 = 750mm$, then this accuracy can be achieved by ensuring that the alignment/calibration accuracy for $\beta \leq 0.14^\circ$ assuming that the other parameters are error free. If ϕ were the only error source, then the same depth error tolerance of $30mm$ can be achieved if $\phi \leq 5.6^\circ$. Similarly, if each of the following parameters were the only source of error then the $30mm$ tolerance in depth accuracy may be achieved if $\theta \leq 9.4^\circ$, $\alpha \leq 9.4^\circ$ and $\kappa \leq 0.0036mm^{-2}$ (assuming κ_1 and κ_2 are equal). For reason of accuracy, all these values are obtained using the exact part of equations 1, 2 and applying the following relations along with the equation which relates y'_2 to y_2 for each case.

$$y_2 = f \frac{Y_2}{D_{tru} + f} \quad (26)$$

and

$$y_1 = f \frac{Y_2 - B}{D_{tru} + f} \quad (27)$$

Consider a reference point at absolute depth D_1 . Due to miscalibration this point is measured at depth $(D_1 + \Delta D_1)$. Consider a second point at absolute depth D_2 , measured as being at depth $(D_2 + \Delta D_2)$. In the error free case, the relative depth is defined to be $(D_2 - D_1)$, and with error it is

$(D_2 - D_1) + (\Delta D_2 - \Delta D_1)$. Hence, error in relative depth is $(\Delta D_2 - \Delta D_1)$. Notice that the relative depth error can be derived from the absolute depth error (which we plot in figure 3 - 11) and is smaller than or equal to the latter (except the lens distortion case). Assume that the reference point is $Y_2 = 0$, and $D_{\text{tru}} = 4000\text{mm}$. Consider another point at $D_{\text{tru}} = 4000\text{mm}$ and $Y_2 = 750\text{mm}$. For these points and the same requirement as before for relative depth accuracy (30mm), the alignment tolerances become: $\beta \leq 11.24^\circ$, $\phi \leq 5.8^\circ$, $\theta \leq 9.4^\circ$, $\alpha \leq 9.4^\circ$ and $\kappa \leq 0.0013\text{mm}^{-2}$. All these parameters are calculated via the same procedure as above for absolute error except here we need to calculate both absolute errors ΔD_2 and ΔD_1 for $Y_2 = 0\text{mm}$ and $Y_2 = 750\text{mm}$. Another practical factor that we need to consider is the spatial quantization of the image plane. For points at distance 4000mm from the cameras, a change in one pixel in the image produces a depth error of 21mm . This means that if misalignment of the different parameters introduces a depth error of no more than 10.5mm then a further improvement in calibration/alignment will not improve the accuracy of depth reconstruction. The accuracy of the vision system is limited by this resolution. Detailed discussion of spatial quantization effects can be found in the literature^[8-10].

2.7 Depth error due to the composition of calibration errors

As mentioned earlier, not only can we analyze the effect of individual calibration errors on 3D measurement accuracy, but we can also analyze the combined effect due to the different error sources - which is more typical in a practical stereo vision system. We can combine the effects of relative roll, pitch, and yaw by consecutively substituting the relationship between y'_2 and y_2 . For example, if the position of misaligned camera can be modeled as being due to the sequence of pitch,

yaw, and roll applied to the ideal camera, then we can combine the follow equations

$$\text{relative roll:} \quad y_2' = y_2 \cos \theta \quad (28)$$

$$\text{relative pitch:} \quad y_2' = y_2 \cos \alpha \quad (29)$$

$$\text{relative yaw:} \quad y_2' = f \frac{y_2 - f \tan \beta}{y_2 \tan \beta + f} \quad (30)$$

to get the final equation for y_2' :

$$y_2' = f \cos \alpha \frac{y_2 \cos \theta - f \tan \beta}{y_2 \cos \theta \tan \beta + f}. \quad (31)$$

Notice here that the order of the motions is very important, and a different order will produce a different result. We can also take the radial lens distortion into account (and for simplicity, we ignore the effect of the tilt in the CCD sensor plane which is usually very small). Using the same sequence of motions and considering lens distortion, we will have the following equations:

$$y_1' = y_1(1 - \kappa_1 y_1^2) \quad (32)$$

$$y_2' = f \cos \alpha \frac{y_2(1 - \kappa_2 y_2^2) \cos \theta - f \tan \beta}{y_2(1 - \kappa_2 y_2^2) \cos \theta \tan \beta + f} \quad (33)$$

$$D_{\text{err}} \simeq D_{\text{tru}} \left(\frac{f \cos \alpha \frac{y_2(1 - \kappa_2 y_2^2) \cos \theta - f \tan \beta}{y_2(1 - \kappa_2 y_2^2) \cos \theta \tan \beta + f} - y_2}{y_2 - y_1} \right) \quad (34)$$

Again similarly to section 2.6, we can compute the parameter error limits for this composite case. For a specified maximum error tolerance for the 3D depth measurement, we would like to know the maximum allowable error for each calibration/alignment parameter. This is obviously an

inverse problem of the *nonlinear* many-to-one relationships derived above. The solution is not easy to obtain and is not unique! An approximation to equation (34) can be written as

$$D_{\text{err-comb}}(\alpha, \beta, \theta, \kappa) \simeq D_{\text{err-roll}}(\alpha) + D_{\text{err-pitch}}(\theta) + D_{\text{err-yaw}}(\beta) + D_{\text{err-lens}}(\kappa) \quad (35)$$

where $D_{\text{err-roll}}$, $D_{\text{err-pitch}}$, $D_{\text{err-yaw}}$, $D_{\text{err-lens}}$ are computed using equations (8), (12), (17), and (25), respectively. Thus, the combined 3D measurement error tolerance $D_{\text{err-comb}}$ is divided into a number of additive components (either arbitrarily or equally) and is allocated to each of the terms on the right hand side of the equation (35). Equations (8), (12), (17), and (25) are then employed (perhaps using look-up tables) to find the corresponding maximum allowable errors in each of the alignment/calibration parameters. Thus, the task is simplified to that of solving, separately, equations of a single variable.

When using the above approximation, we found that the computed parameter tolerances resulted in depth error tolerances that were with $1.5mm$ of the actual, design specification, for the case where the maximum allowable depth error is $120mm$, and if the maximum allowable alignment errors are in the range $\beta \leq 0.14^\circ$, $\theta \leq 9.4^\circ$, $\alpha \leq 9.4^\circ$ and $\kappa \leq 0.0036mm^{-2}$ (assuming κ_1 and κ_2 are equal). Also, we found that within this range, the above approximation will hold irrespective of the order in which the rotations are applied to the ideal camera. The following example illustrates the utility of the above approximation. Consider the first example used in section 2.6, but with errors possible in all parameters (except the tilted CCD). We can distribute the total error to each parameter in different ways – for example, we can assume the equal depth error contribution for each parameter, *i.e.*, $7.5mm$. The individual parameter tolerances are computed to be: $\beta \leq 0.032^\circ$, $\theta \leq 4.5^\circ$, $\alpha \leq 4.5^\circ$ and $\kappa \leq 0.00084mm^{-2}$. Figure 12 illustrates the composite effect of calibration/alignment

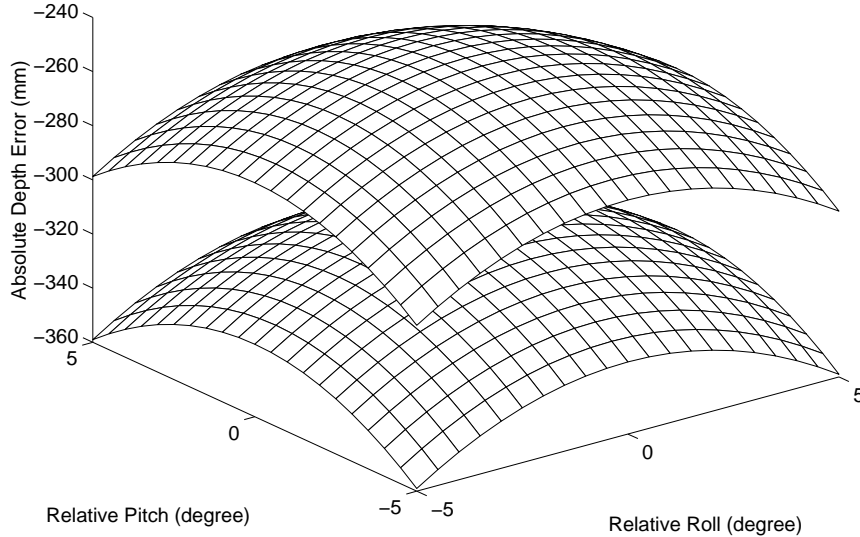


Figure 12: 3D measurement Error due to combination of relative roll, pitch, yaw and lens distortion. The parameters used here are: $B = 1330mm$, $f = 8.5mm$, $Y_2 = 2000mm$, Reference Depth: $4000mm$, and $\kappa_i = 0.00231mm^{-2}$. The upper surface is for $\beta = 0^0$, and the lower surface is for $\beta = 0.2^0$

errors on the 3D measurement accuracy.

3 Experimental Results

A practical stereoscopic vision system (**CCLPS**) has been developed for the reconstruction of surfaces of bulk material such as coal, ore, etc being transported in open rail cars. The computed surfaces are used by environmental scientists to study the cause and effects of loss of the transported material^[14,15]. The data acquisition component of the **CCLPS** system consists of three cameras mounted on a light weight, rigid aluminum bar made up of tubular A-frame sections. The three cameras constitute two wide-baseline, parallel axis stereo pairs which in turn provide wide coverage and high accuracy depth estimates for the sensed scenes.

The camera system was calibrated and aligned in the lab. The greatest accuracy was achieved

by using a collimated laser mounted on an optic table, the motions of the laser being effected on calibrated optical rails and micro positioners. The camera mounts were designed to allow coarse and fine alignment. First, we fixed the cameras loosely on the camera bar. Then we used two tubular rails with carriers to hold the camera bar on the optic table. The laser could move along a rail that was parallel to the camera bar. Thus we could simultaneously calibrate and align the cameras. During calibration, importance was given to those parameters determined to be more critical by the analysis in section 2. After calibration and alignment, the cameras were secured tightly on the camera bar. We found the calibration and alignment to be stable even after several field experiments. Figure 13 shows the actual images sensed by the well-calibrated three-camera rig and the surface reconstructed with correction of camera's lens distortion.

As we showed in equations 8, 12, and 22, we made approximations to the depth errors due to relative roll, pitch and nonparallel configuration of the CCD image plane and the lens. It is important to examine the validity of these relationships that provided guidelines in setting calibration tolerances.

Table 1 shows the difference between the actual D_{ERR} due to relative roll and the approximation to it. Table 2 shows the difference between the actual D_{ERR} introduced by relative pitch and the approximation to it. Table 3 shows the difference between the actual D_{ERR} introduced by nonparallel CCD and lens and the approximation to it. As can be seen the approximations derived for the effects of alignment errors are close to the true values.

As we pointed out earlier, the approximation for depth error due to relative yaw is not as valid as in the previous cases. An example will clarify this: choose a point at depth 4000mm and 3D coordinate $Y2 = 750\text{mm}$ (the yaw angle is 4°), then the true D_{ERR} is -1094mm , and the approximation is -862mm .

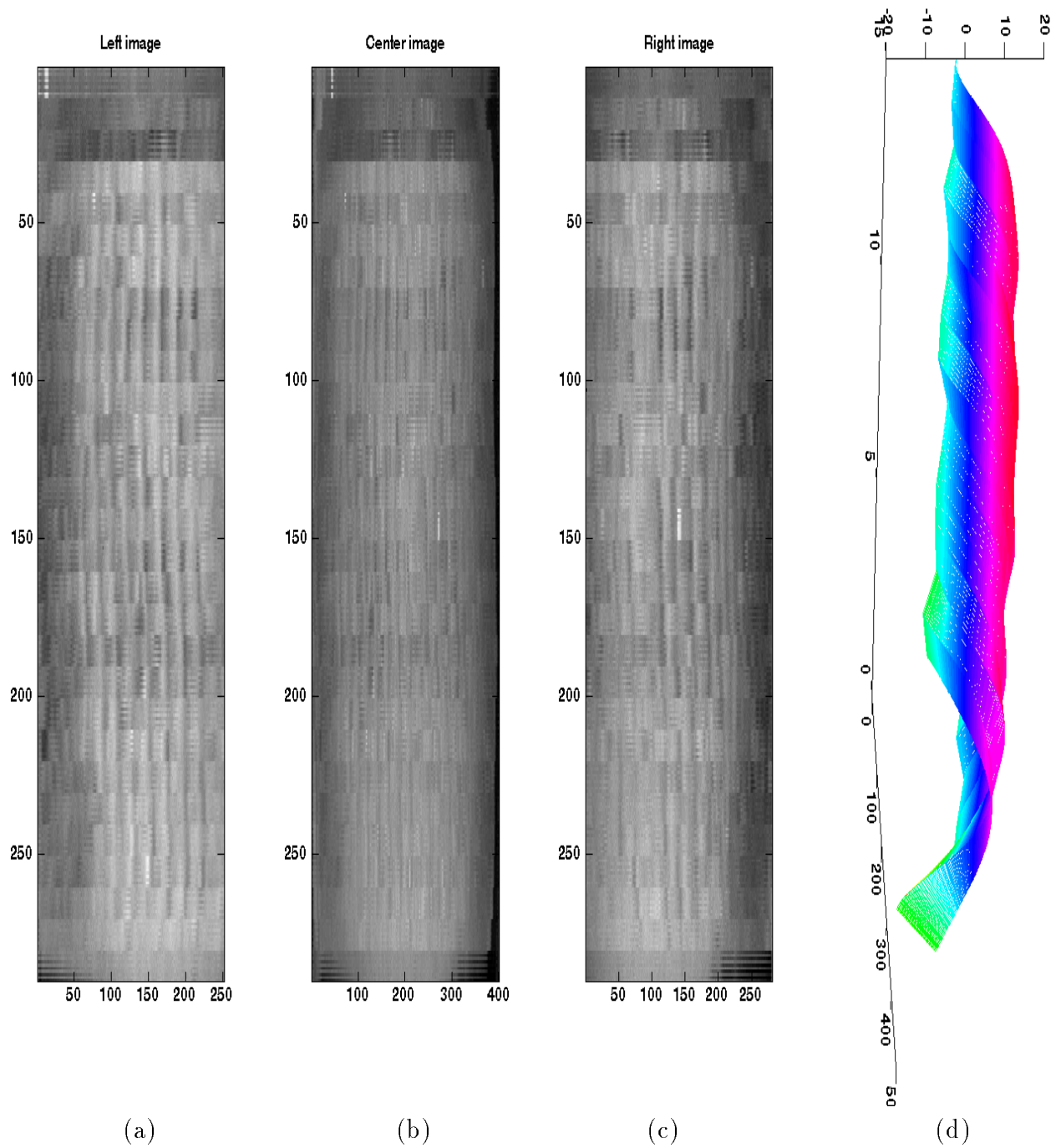


Figure 13: Result from real coal images: (a) Left coal image (b) Center coal image (c) Right coal Image (d) Resulted profiles composed of both halves from two stereoscopic pairs.

$\theta(^{\circ})$	1	2	3	4	5
$RMSD(mm)$	8.40×10^{-5}	1.34×10^{-3}	6.81×10^{-3}	2.1×10^{-2}	5.27×10^{-2}
$RMS_D(mm)$	8.16	7.24	6.17	6.09	8.29

Table 1: Root-mean-square difference (RMSD) between the actual D_{ERR} and the one approximated using equation 8, RMS_D is the root-mean-square value of the D_{ERR} . Other parameters here are the same as those used in figure 3.

$\alpha(^{\circ})$	1	2	3	4	5
$RMSD(mm)$	3.77×10^{-5}	6.03×10^{-4}	3.05×10^{-3}	9.67×10^{-3}	2.36×10^{-2}
$RMS_D(mm)$	8.16	7.24	6.17	6.09	8.29

Table 2: RMSD between the actual D_{ERR} and the one approximated using equation 12. Other parameters here are the same as those used in figure 6.

For lens distortion, we marked 35 points on one wall that was parallel to the camera bar. All cameras had been calibrated and aligned. The distance from the cameras to the wall was 5160mm.

Table 3 shows the importance of considering lens distortion.

4 Conclusion

A quantitative analysis on the relative sensitivity of calibration/alignment parameters on the performance of stereoscopic depth reconstruction was presented. This analysis provides a direct guide for the requirements of these parameters, given error tolerances that the vision system must meet. This analysis not only provides individual parameter error effects, but also describes the composite effect of various sources of error.

$\phi(^{\circ})$	1	2	3	4	5
$RMSD(mm)$	0.444	1.78	4.02	7.15	11.21
$RMS_D(mm)$	16.14	35.22	53.97	71.96	89.13

Table 3: RMSD between the actual D_{ERR} and the one approximated using equation 22. Other parameters here are the same as those used in figure 10.

Point	dis_L	$dcor_L$	dis_R	$dcor_R$	$depth_L$	$depth_R$	$dif(\%)$	$dif_{cor}(\%)$
1	144	144.54	141	147.61	5194.56	5113.48	2.695	1.571
2	145	145.44	141	146.82	5162.27	5140.95	3.392	0.413
3	145	145.40	141	146.15	5163.79	5164.55	3.392	0.015
4	145	145.40	142	146.59	5163.69	5149.02	2.661	0.284
5	145	145.49	143	146.78	5160.55	5142.29	1.941	0.354
6	145	145.59	144	147.36	5156.94	5122.17	1.231	0.674
7	145	145.75	144	146.86	5151.40	5139.41	1.231	0.232
8	145	145.93	144	146.46	5145.07	5153.67	1.231	0.167
9	144	145.17	145	147.05	5171.93	5132.94	0.167	0.755
10	144	145.56	145	146.58	5158.32	5149.21	0.167	0.177
11	143	145.02	146	147.19	5177.58	5127.79	1.564	0.965
12	143	145.64	146	146.85	5155.45	5140.08	1.564	0.298
13	142	145.06	146	146.67	5176.07	5146.31	2.281	0.577
14	141	145.62	147	147.53	5191.85	5116.26	3.689	1.465
15	141	145.23	146	146.43	5169.87	5154.58	3.007	0.296
16	141	145.90	146	146.41	5146.20	5155.56	3.007	0.181
17	140	145.41	146	146.42	5163.57	5154.91	3.745	0.168
18	140	145.95	146	146.47	5144.27	5153.20	3.745	0.174
19	145	145.76	140	146.44	5150.99	5154.33	4.133	0.065
20	145	145.69	140	145.68	5153.66	5181.23	4.133	0.534
21	145	145.66	140	145.15	5154.70	5200.00	4.133	0.879
22	144	144.65	141	145.61	5190.40	5183.37	2.695	0.129
23	145	145.75	142	145.99	5151.42	5170.30	2.661	0.366
24	145	145.87	142	145.46	5147.28	5189.09	2.661	0.810
25	144	145.02	144	147.03	5177.57	5133.56	0.534	0.853
26	145	146.27	143	145.50	5133.18	5187.51	1.941	1.053
27	144	145.49	144	146.14	5160.71	5164.74	0.534	0.078
28	144	145.84	145	146.76	5148.12	5142.93	0.168	0.101
29	144	146.31	145	146.38	5131.67	5156.31	0.168	0.477
30	143	145.84	144	145.03	5148.14	5204.49	0.173	1.092
31	142	145.31	145	145.86	5167.11	5174.88	1.590	0.151
32	142	145.77	145	145.74	5150.85	5179.04	1.590	0.546
33	141	145.25	145	145.65	5169.01	5182.14	2.317	0.256
34	141	146.08	145	145.61	5139.82	5183.77	2.317	0.852
35	140	145.78	145	145.63	5150/49	5182.83	3.054	0.626
Total	$RMS E_{raw}$: 108.9956 (mm)				$RMS E_{cor}$: 19.59 (mm)			

Table 4: Lens distortion’s effect on the 3D measurements: $dis_L(pixel)$ is the measured disparity for left pair, $dcor_L$ is the left disparity after correcting for lens distortion. dis_R and $dcor_R$ are the counterparts for the right pair. $depth_L(mm)$ and $depth_R(mm)$ are the depth derived from the corrected left and right disparities respectively. For each point, we denote dif as the relative difference (percentage) between the distances measured from the left pair and right one without considering the lens distortion. dif_{cor} is the relative difference obtained after using distortion-corrected disparities to calculate distances. $RMS E_{raw}$ is the root-mean-square error of all these points with respect to the true distance using uncorrected measured depth. $RMS E_{cor}$ is the one after using corrected depth. Notice here, the left Baseline and right Baseline are slightly different: $B_{left} = 1325mm$, $B_{right} = 1332mm$

References

- [1] R.M. Haralick and L.G. Shapiro, *Computer and Robot Vision*, vol. II, Addison-Wesley Publishing Company, (1993)
- [2] R.Y. Tsai, A Versatile Camera Calibration Technique for High-Accuracy 3D Machine Vision Metrology Using Off-the-Shelf TV Cameras and Lenses, *IEEE Journal of Robotics and Automation* **RA-3**, 323-344 (1987).
- [3] R.K. Lenz and R.Y. Tsai, Techniques for Calibration of the Scale Factor and Image Center for High Accuracy 3-D Machine Vision Metrology, *IEEE Trans. PAMI* **10**, 713-720 (1988).
- [4] G.Q. Wei and S.D. Ma, Implicit and Explicit Camera Calibration: Theory and Experiments, *IEEE Trans. PAMI* **16**, 469-480 (1994).
- [5] S.W. Shih, Y.P. Hung and W.S. Lin, Accurate Linear technique for camera calibration considering lens distortion by solving an eigenvalue problem, *Optical Engineering* **32**, 138-149, (1993).
- [6] J. Weng, P. Cohen and M. Herniou, Calibration of stereo cameras using a non-linear distortion model, *Proc. IAPR 10th International Conference on Pattern Recognition*, pp. 246-253, (1990).
- [7] T.M. Strat, Recovering the Camera Parameters from a Transformation Matrix, *DARPA Image Understanding Workshop*, pp. 264-271, (1984).
- [8] S.D. Blostein and T.S. Huang, Error Analysis in Stereo Determination of 3-D Point, *IEEE Trans. PAMI* **9**, 752-765 (1987).
- [9] J.J. Rodriguez and J.K. Aggarwal, Stochastic Analysis of Stereo Quantization Error, *IEEE Trans. PAMI* **12**, 467-470 (1990).
- [10] E.S. McVey and J.W. Lee, Some accuracy and Resolution Aspects of Computer Vision Distances Measurements, *IEEE Trans. PAMI* **4**, 646-649, (1982).
- [11] R. Mohan, G. Medioni, and R. Nevatia, Stereo Error Detection, Correction, and Evaluation, *IEEE Trans. PAMI* **11**, 113-120 (1989).
- [12] W. Sohn and N.D. Kehtarnavaz, Analysis of Camera Movement Errors in Vision-Based Vehicle Tracking, *IEEE Trans. PAMI* **17**, 57-61, (1995).
- [13] C.C. Slama, C. Theurer and S.W. Henriksen, *Manual of photogrammetry*, American Society of Photogrammetry, (1980).
- [14] P.W. Smith, N. Nandhakumar, An Automated Stereoscopic Coal Profiling System - CCLPS. *Proc IEEE Workshop on Applications of Computer Vision*, pp. 10-17, (1994).
- [15] W.Y. Zhao, Interpretation of Stereo Imagery of Textured Surfaces, *Master Thesis*, EE Department, University of Virginia, (1995)